JACS
JOURNAL OF THE AMERICAN CHEMICAL SOCIETY

pubs.acs.org/JACS

Communication

Valorization of Click-Based Microporous Organic Polymer: Generation of Mesoionic Carbene−Rh Species for the Stereoselective Synthesis of Poly(arylacetylene)s

Kyoungil Cho, Hee-Seong Yang, In-Hwan Lee, Sang Moon Lee, Hae Jin Kim, and Seung Uk Son*

Cite This: *J. Am. Chem. Soc.* 2021, 143, 4100−4105

Read Online

ACCESS | Metrics & More | Article Recommendations | Supporting Information

ABSTRACT: This work reports the functionalization of azide−alkyne click-based microporous organic polymer (CMOP). The generation of triazolium salts and successive deprotonation induced mesoionic carbene species in hollow CMOP (H-CMOP). Rh(I) species could be coordinated to the mesoionic carbene species to form H-CMOP-Rh, showing excellent heterogeneous catalytic performance in the stereoselective polymerization of arylacetylenes.

Downloaded via UNIV OF CALIFORNIA SANTA BARBARA on May 15, 2021 at 00:03:25 (UTC).
See https://pubs.acs.org/sharingguidelines for options on how to legitimately share published articles.

The azide−alkyne Huisgen [3 + 2] cycloaddition is a versatile reaction for organic synthesis.[1] Because the reaction was referred to as an example of click chemistry by Sharpless in 2001, its application fields have expanded to the engineering of functional materials.[2−4]

Recently, microporous organic polymer (MOP) has been prepared by various coupling reactions of organic building blocks.[5−13] The azide−alkyne click reaction has also been applied to the synthesis of MOP.[14−20] Huang et al. showed that Cu_2O can be used as a catalyst for the azide−alkyne click reaction.[21] Our research group has shown that hollow MOP could be synthesized through Cu_2O-based template synthesis.[19,20] The resultant MOPs are rich in 1,2,3-triazoles. A delicate postsynthetic modification (PSM) approach can be further applied to generate more advanced chemical species in the click-based MOP (CMOP).

1,2,3-Triazole compounds can be converted to triazolium species through a reaction with electrophiles.[22,23] The triazolium rings are used as precursors to generate mesoionic carbenes through the abstraction of protons.[22,23] Recently, the mesoionic carbenes have been utilized in the synthesis of metal−carbene complexes.[24−27] For example, a reaction of the mesoionic carbene derived from 3-methyl-1,4-diphenyl-1,2,3-triazolium iodide with $[Rh(COD)Cl]_2$, (COD: 1,5-cyclooctadiene) generates the Model-Rh complex (Figure S1).

In 2011, we reported the synthesis of MOP bearing imidazolium salts through a predesigned building block approach.[28] Imidazolium moieties could be utilized for the generation of N-heterocyclic carbene−metal species in polymeric materials.[29−34] However, in spite of the usefulness of azide−alkyne click reactions, as far as we are aware, the generation of mesoionic carbene−metal species in CMOP has not been reported. In this work, we report the generation of mesoionic abnormal carbenes in hollow CMOP (H-CMOP), successive incorporation of Rh species, and its heterogeneous catalytic performance in the stereoselective synthesis of poly(arylacetylene)s.

Figure 1 shows a synthetic scheme of H-CMOP bearing mesoionic carbene−Rh species (H-CMOP-Rh). First, Cu_2O nanocubes were prepared by a literature method.[21] Then, CMOP was formed on the surface of templating Cu_2O nanocubes. The acid etching of Cu_2O@CMOP resulted in H-CMOP. The reaction with methyl iodide generated H-CMOP with triazoliums (H-CMOP-Me). Finally, abstraction of proton from triazoliums and successive reaction with $[Rh(COD)Cl]_2$ resulted in H-CMOP-Rh.

Scanning and transmission electron microscopy (SEM and TEM) showed the hollow morphologies of H-CMOP with a diameter and a shell thickness of 110 and 20 nm, respectively (Figures 2a and 2d). The H-CMOP-Me and H-CMOP-Rh maintained the original hollow morphologies (Figures 2b,c and 2e,f).

The porosity and surface area of H-CMOPs were characterized by N_2 sorption studies (Figure 3a,b and Table S1). While the surface area of H-CMOP was measured to be 422 m^2/g, that of H-CMOP-Me was reduced to 167 m^2/g due to the incorporation of additional chemical component. After the coordination of Rh, the surface area of H-CMOP-Rh significantly increased to 310 m^2/g, which is attributable to the enhanced rigidity of network structure (Figure 3c). All CMOPs in this work were amorphous (Figure S2). It has been reported[35,36] that metal coordination to the relatively flexible network structure of MOPs enhanced the porosity. In addition, the further networking by Rh catalysis during PSM cannot be ruled out.[37−40] The pore size distribution analysis indicated the microporosity of H-CMOP, H-CMOP-Me, and H-CMOP-Rh with pore volumes of 0.58, 0.28, and 0.55 cm^3/g, respectively (Figure 3b). Interestingly, the significant macro/

Received: December 27, 2020
Published: March 9, 2021

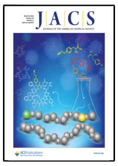

© 2021 American Chemical Society

https://dx.doi.org/10.1021/jacs.0c13286

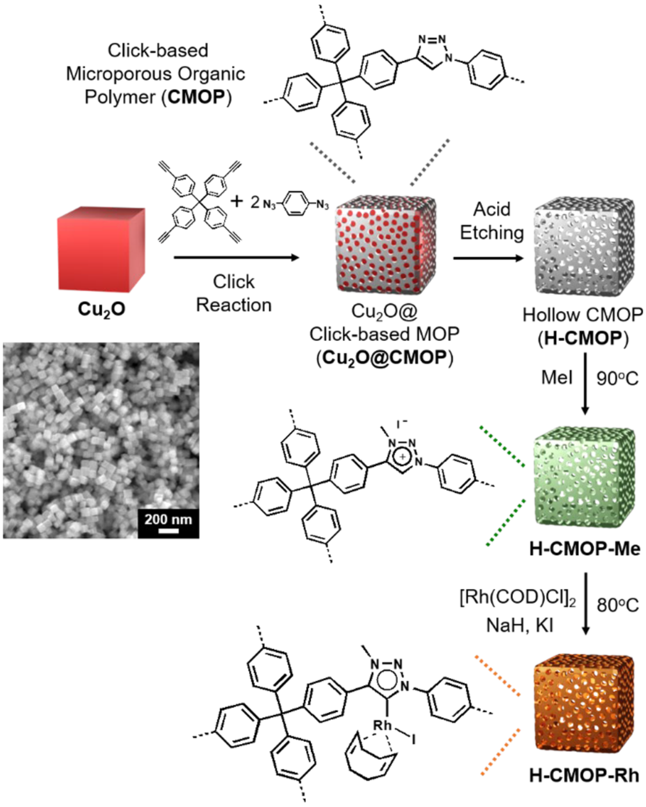

Figure 1. Synthesis of H-CMOP-Rh and a SEM image of Cu_2O nanocubes.

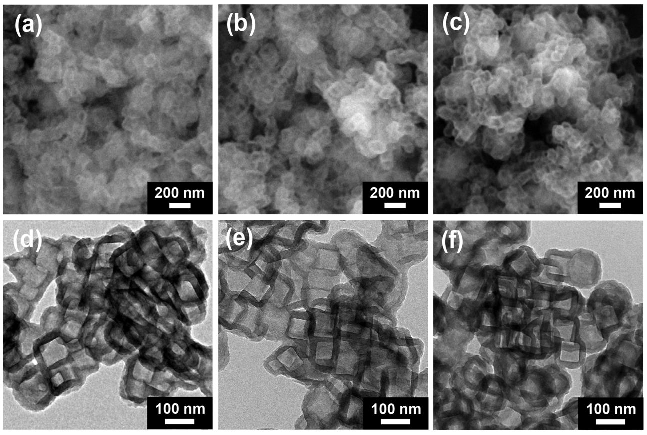

Figure 2. SEM and TEM images of (a, d) H-CMOP, (b, e) H-CMOP-Me, and (c, f) H-CMOP-Rh.

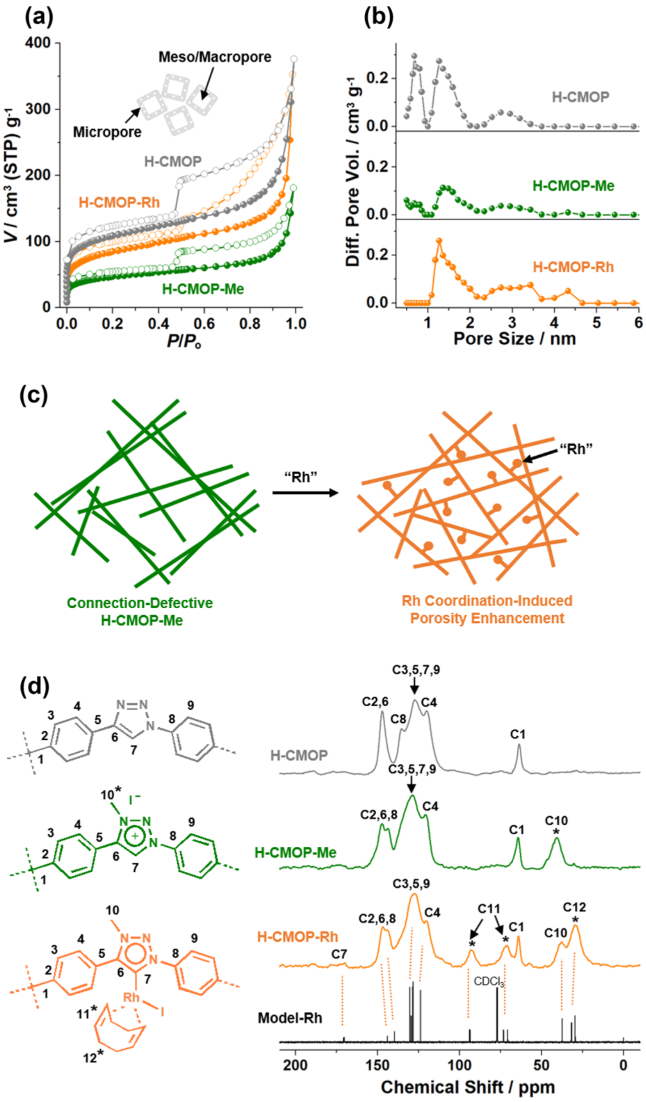

Figure 3. (a) N_2 sorption isotherm curves at 77K, (b) pore size distribution diagrams, (c) the porosity enhancement of H-CMOP-Rh through Rh coordination, and (d) ^{13}C NMR spectra of H-CMOP, H-CMOP-Me, H-CMOP-Rh, and Model-Rh.

mesoporosity was also observed over all H-CMOPs, which is attributable to the inner hollow cube space (Figure 3a and Figure S3).

The chemical structures of H-CMOPs were characterized by solid-state ^{13}C nuclear magnetic resonance (NMR) spectroscopy (Figure 3d). While the ^{13}C peak of benzylic carbon in H-CMOP appeared at 64 ppm, aromatic ^{13}C peaks were observed at 110−140 and 147 ppm. The alkyne ^{13}C NMR peaks were not observed at 70−90 ppm, indicating that the azide−alkyne reaction was successfully conducted. In comparison, the methyl ^{13}C peak of H-CMOP-Me was clearly observed at 41 ppm. In addition, the *N*-phenyl ^{13}C peak of 1,2,3-triazoles shifted from 135 ppm (H-CMOP) to 144 ppm (H-CMOP-Me) due to the formation of cationic triazoliums. The ^{13}C peaks of COD in the H-CMOP-Rh were clearly observed at 29, 72, and 93 ppm, matching with those of Model-Rh (Figure 3d and Figure S4). In the infrared absorption (IR) spectra of H-CMOP, H-CMOP-Me, and H-CMOP-Rh, aromatic C═C vibration peaks were observed at 1483, 1522, and 1608 cm^{-1}, in addition to aromatic C−H peaks at 832 and 989−1034 cm^{-1}. The H-CMOP-Rh showed additional aliphatic C−H vibration peaks of the COD at 2822, 2879, and 2921 cm^{-1} (Figure S5).

The mesoionic carbene Rh species in the H-CMOP-Rh were further characterized by X-ray photoelectron spectroscopy (XPS) (Figures S4 and S6). The major N 1s orbital peak of the triazole rings of H-CMOP appeared at 399.7 eV with a minor peak at 401.3 eV. In comparison, the major N 1s orbital peak of the triazolium rings of H-CMOP-Me was observed at 401.4 eV with an additional peak at 399.9 eV. In the case of H-CMOP-Rh, the major N 1s orbital peak was shifted to 401.7 eV, matching with that (401.7 eV) of Model-Rh. The 3d orbital peaks of Rh in H-CMOP-Rh were observed at 312.6 and 307.9 eV, matching with those of the Model-Rh at 312.4

and 307.7 eV. While the 3d orbital peaks of iodides in H-CMOP-Me were observed at 631.8 and 620.5 eV, those of the iodo ligands in H-CMOP-Rh shifted to 630.4 and 618.5 eV. In comparison, the 3d orbital peaks of iodo ligands in the Model-Rh were observed at 630.1 and 618.8 eV. Energy-dispersive X-ray spectroscopy-based elemental mapping confirmed the homogeneous distribution of Rh species in H-CMOP-Rh (Figure S6).

The amounts of triazoles, triazoliums, and mesoionic carbenes in H-CMOP, H-CMOP-Me, and H-CMOP-Rh were analyzed to be 3.76 mmol/g (15.8 wt % N), 3.16 mmol/g (13.3 wt % N), and 2.2 mmol/g (9.3 wt % N), respectively. The Cu residues in H-CMOP were measured to be 0.28 wt % by inductively coupled plasma (ICP) analysis. The content of Rh in H-CMOP-Rh was measured to be 8.63 wt % (0.849 mmol/g), corresponding to the 38% PSM of triazoliums. Thermogravimetric analysis showed that the H-CMOP-Rh is stable up to 228 °C (Figure S7).

Considering the mesoionic carbene−Rh species and chemical stability of H-CMOP-Rh, we studied its heterogeneous catalytic activities in the polymerization of arylacetylenes (Table 1). Recently, poly(phenylacetylene) (PPA) has attracted the significant attention of scientists.[37−42] While the PPA has been prepared by various metal catalysts, Rh complexes have shown high synthetic efficiencies.[43−46] However, Rh-based heterogeneous catalytic systems are relatively rare.[47−51]

Table 1. Synthesis of Poly(Arylacetylene)s by H-CMOP-Rh[a]

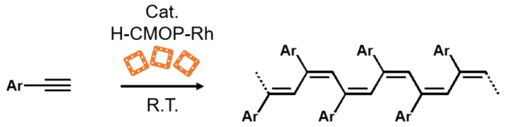

entry	Ar	cat. (mol %)	yield[b] (S[c]) (%)	M_n	PDI
1	Ph	1.2	99 (99)	32100	2.59
2	Ph	0.60	96 (98)	40900	2.47
3	Ph	0.30	76 (98)	41300	2.51
4	Ph	0.12	64 (99)	42800	2.76
5	Ph	0.060	24 (99)	39300	2.84
6[d]	Ph	0.60	92 (99)	42200	2.70
7[e]	Ph	0.60	96 (96)	48400	2.53
8[f]	Ph	0.60	94 (96)	50500	2.34
9[g]	Ph	0.60	91 (99)	54100	2.33
10	4-BrPh	0.60	89 (–[h])	–[h]	–[h]
11	4-BrPh:Ph (1:1)	0.60	70[i] (96)	35200	3.04
12	4-MeOPh	0.60	3 (96)	5700	2.01
13	4-MeOPh:Ph (5:1)	0.60	21[j] (99)	6000	1.92
14	4-MeOPh:Ph (1:1)	0.60	85[k] (96)	21100	2.24
15[l]	Ph	0.60	37 (86)	21000	2.37

[a]Reaction conditions: arylacetylene (2.28 mmol), H-CMOP-Rh (16 mg for 0.60 mol % Rh), rt, THF, 18 h. [b]Isolated yield. [c]Contents of *cis-transoid* polymers.[52] [d]The catalyst recovered from entry 2 was used. [e]The catalyst recovered from entry 6 was used. [f]The catalyst recovered from entry 7 was used. [g]The catalyst recovered from entry 8 was used. [h]Insoluble polymers were obtained. [i]The 1:1.18 ratio of 4-bromophenyl and phenyl in copolymer. [j]The 1:0.21 ratio of 4-methoxyphenyl and phenyl in copolymer. [k]The 1:1.39 ratio of 4-methoxyphenyl and phenyl in copolymer. [l]Nonhollow CMOP-Rh (34 mg for 0.60 mol % Rh) was used.

First, we scanned the amount of catalyst. As the amount of H-CMOP-Rh decreased from 1.2 mol % Rh to 0.60, 0.30, 0.12, and 0.060 mol % Rh, the isolated yields of PPAs decreased from 99% to 96, 76, 64, and 24% with the changes of molecular weights (M_n) from 32100 to 40900, 41300, 42800, and 39300, respectively (entries 1−5 in Table 1). The stereoselectivities of *cis-transoid* PPA were analyzed to be 98−99%.[52] We selected the 0.60 mol % H-CMOP-Rh as an optimal catalyst amount. In a control test, 0.60 mol % Model-Rh showed a 10% isolated yield of PPA. The enhanced polymerization of phenylacetylene in nanospaces[53,54] and the extrusion polymerization by mesoporous catalysts have been reported.[55]

The H-CMOP-Rh (0.60 mol % Rh) could be recycled. When the recovered H-CMOP-Rh was used, the PPAs were obtained with the isolated yields of 92, 96, 94, and 91% and the M_n values of 42200, 48400, 50500, and 54100 at the 2nd, 3rd, 4th, and 5th runs, respectively (entries 6−9 in Table 1). After the removal of H-CMOP-Rh through filtration, the Rh was not detected in the reaction mixture and the reaction did not proceed, indicating the heterogeneous nature of the catalytic reactions (Figure S8). SEM, TEM, XPS, IR, and ^{13}C NMR studies of the H-CMOP-Rh recovered after the fifth reaction showed that the original hollow morphologies and mesoionic carbene Rh species were retained (Figure S9).

Next, we studied the polymerization of arylacetylenes bearing substituents. When we used (4-bromophenyl)-acetylene, insoluble polymer was obtained (entry 10 in Table 1, Figure S10). When we used a 1:1 mixture of (4-bromophenyl)acetylene and phenylacetylene, soluble polymer (M_n of 35200) was obtained with an isolated yield of 70% (entry 11 in Table 1, Figure S11). In comparison, when we used the (4-methoxyphenyl)acetylene, polymer was obtained with a yield of 3% (M_n of 5700) (entry 12 in Table 1). We suggest that the different activities of H-CMOP-Rh toward (4-bromophenyl)acetylene and (4-methoxyphenyl)acetylene result from an initiation step of polymerization. Recently, Morokuma et al. reported mechanistic studies of the Rh-catalyzed polymerization of phenylacetylene.[56] Among three mechanistic candidates—Rh(I) insertion, Rh(III) insertion, and Rh−carbene metathesis mechanisms—the Rh(I) insertion was suggested as the most favorable pathway. In this regard, the catalytic mechanism of H-CMOP-Rh is suggested in Figure S12. To initiate the polymerization, the anionic arylethynyl ligand should be incorporated into Rh through the deprotonation of arylacetylene. We speculate that the initiation of polymerization by (4-methoxyphenyl)acetylene would be relatively slow due to its relatively less acidic feature of the terminal proton.

When we used the 5:1 and 1:1 mixtures of (4-methoxyphenyl)acetylene and phenylacetylene as monomer systems, the isolated yields of polymer increased to 21% (M_n of 6000) and 85% (M_n of 21100), respectively (entries 13 and 14 in Table 1, Figure S11).

While the features of PPA have been extensively investigated, the copolymers bearing substituted arylacetylenes have been relatively less explored.[57−59] In this regard, the optical properties of PPA, copolymer of (4-bromophenyl)-acetylene and phenylacetylene (PBrPAPA), and copolymer of (4-methoxyphenyl)acetylene and phenylacetylene (PMeOPAPA) were studied (Figure S11). While the PPA and the PMeOPAPA showed two absorption bands at 328 and 388 nm, the absorptions of the PBrPAPA at 320−400 nm were significantly reduced. Interestingly, the emissions of PBrPAPA and PMeOPAPA at 494 and 510 nm, respectively, were significantly enhanced by 8.8 and 6.6 times compared with that of PPA at 511 nm. The polymer chains of PPA are known to form a helical structure.[37−46,57−59] We speculate that the existence of substituents in phenyl rings hinders the $\pi-\pi$ stacking-induced emission quenching between polymer chains, resulting in the enhanced emission.

Finally, when we conducted control studies for the nontemplate synthesis of CMOP, conventional nonhollow spherical materials (denoted as CMOP-Rh) were obtained with diameters of 0.2−0.7 μm, a Rh content of 4.13 wt %, and a surface area of 147 m^2/g (Figure S13). In polymerization studies, the CMOP-Rh (0.60 mol % Rh) produced PPA (M_n: 21000) with an isolated yield of 37% and a *cis-transoid* content of 86% (entry 15 in Table 1), indicating that the hollow structure and the thin shell of H-CMOP and H-CMOP-Rh are beneficial in the postsynthetic functionalization and catalytic performance due to the reduced diffusion pathways of reagents into materials.[60]

In conclusion, this work shows that CMOP can be chemically valorized to mesoionic carbene donor materials. The Rh coordination to the mesoionic carbene moieties in the CMOP resulted in a heterogeneous catalyst sytem, showing excellent catalytic activities in the stereoselective synthesis of PPA and copolymers. In addition, the H-CMOP-Rh could be reused in five successive reactions. We believe that the H-CMOP-Rh can be applied to various catalytic reactions,[25−27] and the chemistry of this work is generally applicable to various MOPs containing triazole rings.

■ ASSOCIATED CONTENT

Supporting Information

The Supporting Information is available free of charge at https://pubs.acs.org/doi/10.1021/jacs.0c13286.

> Experimental procedure, additional characterization of H-CMOP-Rh, and characterization data of recycled H-CMOP-Rh and nonhollow CMOP-Rh (PDF)

■ AUTHOR INFORMATION

Corresponding Author

Seung Uk Son − *Department of Chemistry, Sungkyunkwan University, Suwon 16419, Korea;* orcid.org/0000-0002-4779-9302; Email: sson@skku.edu

Authors

Kyoungil Cho − *Department of Chemistry, Sungkyunkwan University, Suwon 16419, Korea;* orcid.org/0000-0003-2506-4951

Hee-Seong Yang − *Department of Energy System Research, Ajou University, Suwon 16499, Korea*

In-Hwan Lee − *Department of Chemistry, Ajou University, Suwon 16499, Korea;* orcid.org/0000-0002-4848-939X

Sang Moon Lee − *Korea Basic Science Institute, Daejeon 34133, Korea*

Hae Jin Kim − *Korea Basic Science Institute, Daejeon 34133, Korea;* orcid.org/0000-0002-1960-0650

Complete contact information is available at: https://pubs.acs.org/10.1021/jacs.0c13286

Notes

The authors declare no competing financial interest.

■ ACKNOWLEDGMENTS

This work was supported by “Carbon to X Project” (No. 2020M3H7A1098283) and Grant 2020R1A2C2004310 through the National Research Foundation (NRF) funded by the Ministry of Science and ICT, Republic of Korea.

■ REFERENCES

(1) Huisgen, R. 1,3-Dipolar cycloadditions. *Proc. Chem. Soc.* **1961**, 357−396.

(2) Kolb, H. C.; Finn, M. G.; Sharpless, K. B. Click chemistry: diverse chemical function from a few good reactions. *Angew. Chem., Int. Ed.* **2001**, *40*, 2004−2021.

(3) Meldal, M.; Tornøe, C. W. Cu-catalyzed azide-alkyne cycloaddition. *Chem. Rev.* **2008**, *108*, 2952−3015.

(4) Golas, P. L.; Matyjaszewski, K. Marrying click chemistry with polymerization: expanding the scope of polymeric materials. *Chem. Soc. Rev.* **2010**, *39*, 1338−1354.

(5) Lee, J. -S. M.; Cooper, A. I. Advances in conjugated microporous polymers. *Chem. Rev.* **2020**, *120*, 2171−2214.

(6) Zheng, B.; Lin, X.; Zhang, X.; Wu, D.; Matyjaszewski, K. Emerging functional porous polymeric and carbonaceous materials for environmental treatment and energy storage. *Adv. Funct. Mater.* **2020**, *30*, 1907006.

(7) Chaoui, N.; Trunk, M.; Dawson, R.; Schmidt, J.; Thomas, A. Trends and challenges for microporous polymers. *Chem. Soc. Rev.* **2017**, *46*, 3302−3321.

(8) Tan, L.; Tan, B. Hypercrosslinked porous polymer materials: design, synthesis, and applications. *Chem. Soc. Rev.* **2017**, *46*, 3322−3356.

(9) Das, S.; Heasman, P.; Ben, T.; Qiu, S. Porous organic materials: strategic design and structure-function correlation. *Chem. Rev.* **2017**, *117*, 1515−1563.

(10) Sun, J.-K.; Antonietti, M.; Yuan, J. Nanoporous ionic organic networks: from synthesis to materials applications. *Chem. Soc. Rev.* **2016**, *45*, 6627−6656.

(11) Xu, Y.; Jin, S.; Xu, H.; Nagai, A.; Jiang, D. Conjugated microporous polymers: design, synthesis and application. *Chem. Soc. Rev.* **2013**, *42*, 8012−8031.

(12) Vilela, F.; Zhang, K.; Antonietti, M. Conjugated porous polymers for energy applications. *Energy Environ. Sci.* **2012**, *5*, 7819−7832.

(13) Kang, N.; Park, J. H.; Jin, M.; Park, N.; Lee, S. M.; Kim, H. J.; Kim, J. M.; Son, S. U. Microporous organic network hollow spheres: useful templates for nanoparticulate Co_3O_4 hollow oxidation catalysts. *J. Am. Chem. Soc.* **2013**, *135*, 19115−19118.

(14) Holst, J. R.; Stöckel, E.; Adams, D. J.; Cooper, A. I. High Surface area networks from tetrahedral monomers: metal-catalyzed coupling, thermal polymerization, and “click” chemistry. *Macromolecules* **2010**, *43*, 8531−8538.

(15) Pandey, P.; Farha, O. K.; Spokoyny, A. M.; Mirkin, C. A.; Kanatzidis, M. G.; Hupp, J. T.; Nguyen, S. T. A “click-based” porous organic polymer from tetrahedral building blocks. *J. Mater. Chem.* **2011**, *21*, 1700−1703.

(16) Plietzsch, O.; Schilling, C. I.; Grab, T.; Grage, S. L.; Ulrich, A. S.; Comotti, A.; Sozzani, P.; Muller, T.; Bräse, S. Click chemistry produces hyper-cross-linked polymers with tetrahedral cores. *New J. Chem.* **2011**, *35*, 1577−1581.

(17) Li, L.; Zhao, H.; Wang, R. Tailorable synthesis of porous organic polymers decorating ultrafine palladium nanoparticles for hydrogenation of Olefins. *ACS Catal.* **2015**, *5*, 948−955.

(18) Li, L.; Cui, C.; Su, W.; Wang, Y.; Wang, R. Hollow click-based porous organic polymers for heterogenization of $[Ru(bpy)^3]^{2+}$ through electrostatic interactions. *Nano Res.* **2016**, *9*, 779−786.

(19) Kang, D.; Ko, J. H.; Choi, J.; Cho, K.; Lee, S. M.; Kim, H. J.; Ko, Y.-J.; Park, K. H.; Son, S. U. Dual role of Cu_2O nanocubes as templates and networking catalysts for hollow and microporous Fe-porphyrin networks. *Chem. Commun.* **2017**, *53*, 2598−2601.

(20) Lee, J.; Choi, J.; Kang, D.; Myung, Y.; Lee, S. M.; Kim, H. J.; Ko, Y.-J.; Kim, S.-K.; Son, S. U. Thin and small N-doped carbon boxes obtained from microporous organic networks and their excellent energy storage performance at high current densities in coin cell supercapacitors. *ACS Sustainable Chem. Eng.* **2018**, *6*, 3525−3532.

(21) Tsai, Y.-H.; Chanda, K.; Chu, Y.-T.; Chiu, C.-Y.; Huang, M. H. Direct formation of small Cu_2O nanocubes, octahedra, and octapods for efficient synthesis of triazoles. *Nanoscale* **2014**, *6*, 8704−8709.

(22) Vivancos, A.; Segarra, C.; Albrecht, M. Mesoionic and related less heteroatom-stabilized N-heterocyclic carbene complexes: synthesis, catalysis, and other applications. *Chem. Rev.* **2018**, *118*, 9493−9586.

(23) Guisado-Barrios, G.; Bouffard, J.; Donnadieu, B.; Bertrand, G. Crystalline 1H-1,2,3-triazol-5-ylidenes: new stable mesoionic carbenes (MICs). *Angew. Chem., Int. Ed.* **2010**, *49*, 4759−4762.

(24) Poulain, A.; Canseco-Gonzalez, D.; Hynes-Roche, R.; Müller-Bunz, H.; Schuster, O.; Stoeckli-Evans, H.; Neels, A.; Albrecht, M. Synthesis and tunability of abnormal 1,2,3-triazolylidene palladium and rhodium complexes. *Organometallics* **2011**, *30*, 1021−1029.

(25) Saravanakumar, R.; Ramkumar, V.; Sankararaman, S. Synthesis and structure of 1,4-diphenyl-3-methyl-1,2,3-triazol-5-ylidene palladium complexes and application in catalytic hydroarylation of alkynes. *Organometallics* **2011**, *30*, 1689−1694.

(26) Donnelly, K. F.; Lalrempuia, R.; Müller-Bunz, H.; Albrecht, M. Regioselective electrophilic C-H bond activation in triazolylidene metal complexes containing a N-bound phenyl substituent. *Organometallics* **2012**, *31*, 8414−8419.

(27) Sánchez-Page, B.; Jiménez, M. V.; Pérez-Torrente, J. J.; Passarelli, V.; Blasco, J.; Subias, G.; Granda, M.; Alvarez, P. Hybrid catalysts composed of graphene modified with rhodium-based N-heterocyclic carbenes for alkyne hydrosilylation. *ACS Appl. Nano Mater.* **2020**, *3*, 1640−1655.

(28) Cho, H. C.; Lee, H. S.; Chun, J.; Lee, S. M.; Kim, H. J.; Son, S. U. Tubular microporous organic networks bearing imidazolium salts and their catalytic CO_2 conversion to cyclic carbonates. *Chem. Commun.* **2011**, *47*, 917−919.

(29) Wang, W.; Zheng, A.; Zhao, P.; Xia, C.; Li, F. Au-NHC@ porous organic polymers: synthetic control and its catalytic application in alkyne hydration reactions. *ACS Catal.* **2014**, *4*, 321−327.

(30) Lin, M.; Wang, S.; Zhang, J.; Luo, W.; Liu, H.; Wang, W.; Su, C.-Y. Guest uptake and heterogeneous catalysis of a porous Pd(II) N-heterocyclic carbene polymer. *J. Mol. Catal. A: Chem.* **2014**, *394*, 33−39.

(31) Talapaneni, S. N.; Buyukcakir, O.; Je, S. H.; Srinivasan, S.; Seo, Y.; Polychronopoulou, K.; Coskun, A. Nanoporous polymers incorporating sterically confined N-heterocyclic carbenes for simultaneous CO_2 Capture and conversion at ambient pressure. *Chem. Mater.* **2015**, *27*, 6818−6826.

(32) Su, Y.; Wang, Y.; Li, X.; Li, X.; Wang, R. Imidazolium-based porous organic polymers: anion exchange-driven capture and luminescent probe of $Cr_2O_7^{2-}$. *ACS Appl. Mater. Interfaces* **2016**, *8*, 18904−18911.

(33) Hao, S.; Liu, Y.; Shang, C.; Liang, Z.; Yu, J. CO_2 adsorption and catalytic application of imidazole ionic liquid functionalized porous organic polymers. *Polym. Chem.* **2017**, *8*, 1833−1839.

(34) Liu, Z.-W.; Cao, C.-X.; Han, B.-H. A cationic porous organic polymer for high-capacity, fast, and selective capture of anionic pollutants. *J. Hazard. Mater.* **2019**, *367*, 348−355.

(35) Xie, Y.; Wang, T.-T.; Liu, X.-H.; Zou, K.; Deng, W.-Q. Capture and conversion of CO_2 at ambient conditions by a conjugated microporous polymer. *Nat. Commun.* **2013**, *4*, 1960.

(36) Cho, K.; Lee, S. M.; Kim, H. J.; Ko, Y.-J.; Kang, E. J.; Son, S. U. Iron coordination to hollow microporous metal-free disalphen networks: heterogeneous iron catalysts for CO_2 fixation to cyclic carbonates. *Chem. - Eur. J.* **2020**, *26*, 788−794.

(37) Grundy, M.; Ye, Z. Cross-linked polymers of diethynylbenzene and phenylacetylene as new polymer precursors for high-yield synthesis of high-performance nanoporous activated carbons for supercapacitors, hydrogen storage, and CO_2 capture. *J. Mater. Chem. A* **2014**, *2*, 20316−20330.

(38) Sedláček, J.; Balcar, H. Substituted polyacetylenes prepared with Rh catalysts: from linear to network-type conjugated polymers. *Polym. Rev.* **2017**, *57*, 31−51.

(39) Sekerová, L.; Lhotka, M.; Vyskočilová, E.; Faukner, T.; Slováková, E.; Brus, J.; Červený, L.; Sedláček, J. Hyper-cross-linked polyacetylene-type microporous networks decorated with terminal ethynyl groups as heterogeneous acid catalysts for acetalization and esterification reactions. *Chem. - Eur. J.* **2018**, *24*, 14742−14749.

(40) Havelkova, L.; Haskova, A.; Bashta, B.; Brus, J.; Lhotka, M.; Vrbkova, E.; Kindl, M.; Vyskočilová, E.; Sedlacek, J. Synthesis of hyper-cross-linked microporous poly(phenylacetylene)s having aldehyde and other groups and their chemisorption and physisorption ability. *Eur. Polym. J.* **2019**, *114*, 279−286.

(41) Tan, N. S. L.; Lowe, A. B. Polymerizations mediated by well-defined rhodium complexes. *Angew. Chem., Int. Ed.* **2020**, *59*, 5008−5021.

(42) Yashima, E.; Ousaka, N.; Taura, D.; Shimomura, K.; Ikai, T.; Maeda, K. Supramolecular helical systems: helical assemblies of small molecules, foldamers, and polymers with chiral amplification and their functions. *Chem. Rev.* **2016**, *116*, 13752−13990.

(43) Kishimoto, Y.; Eckerle, P.; Miyatake, T.; Ikariya, T.; Noyori, R. Living polymerization of phenylacetylenes initiated by $Rh(CCC_6H_5)$-(2,5-norbornadiene)$[P(C_6H_5)_3]_2$. *J. Am. Chem. Soc.* **1994**, *116*, 12131−13132.

(44) Tang, B. Z.; Poon, W. H.; Leung, S. M.; Leung, W. H.; Peng, H. Synthesis of stereoregular poly(phenylacetylene)s by organorhodium complexes in aqueous media. *Macromolecules* **1997**, *30*, 2209−2212.

(45) Angoy, M.; Jiménez, M. V.; García-Orduna, P.; Oro, L. A.; Vispe, E.; Pérez-Torrente, J. J. Dinuclear phosphine-amido $[Rh_2(diene)\{\mu\text{-}NH(CH_2)_3PPh_2\}_2]$ complexes as efficient catalyst precursors for phenylacetylene polymerization. *Organometallics* **2019**, *38*, 1991−2006.

(46) Tan, N. S. L.; Nealon, G. L.; Turner, G. F.; Moggach, S. A.; Ogden, M. I.; Massi, M.; Lowe, A. B. Rh(I)(2,5-norbornadiene)-(biphenyl)(tris(4-fluorophenyl)phosphine): synthesis, characterization, and application as an initiator in the stereoregular (co)-polymerization of phenylacetylenes. *ACS Macro Lett.* **2020**, *9*, 56−60.

(47) Balcar, H.; Sedláček, J.; Čejka, J. Vohlídal, MCM-41-Immobilized $[Rh(cod)OCH_3]_2$ complex-a hybrid catalyst for the polymerization of phenylacetylene and its ring-substituted derivatives. *Macromol. Rapid Commun.* **2002**, *23*, 32−37.

(48) Park, K. H.; Jang, K.; Son, S. U.; Sweigart, D. A. Self-supported organometallic rhodium quinonoid nanocatalysts for stereoselective polymerization of phenylacetylene. *J. Am. Chem. Soc.* **2006**, *128*, 8740−8741.

(49) Abe, S.; Hirata, K.; Ueno, T.; Morino, K.; Shimizu, N.; Yamamoto, M.; Takata, M.; Yashima, E.; Watanabe, Y. Polymerization of phenylacetylene by rhodium complexes within a discrete space of apo-ferritin. *J. Am. Chem. Soc.* **2009**, *131*, 6958−6960.

(50) Grimm, A. R.; Sauer, D. F.; Polen, T.; Zhu, L.; Hayashi, T.; Okuda, J.; Schwaneberg, U. A whole cell E. coli display platform for artificial metalloenzymes: poly(phenylacetylene) production with a rhodium-nitrobindin metalloprotein. *ACS Catal.* **2018**, *8*, 2611−2614.

(51) Zhang, L.; Cao, Q.; Gao, F.; Dong, Y.; Li, X. Self-supported rhodium catalysts based on a microporous metal-organic framework for polymerization of phenylacetylene and its derivatives. *Polym. Chem.* **2020**, *11*, 2904−2913.

(52) Tabata, M.; Sone, T.; Sadahiro, Y. Precise synthesis of monosubstituted polyacetylenes using Rh complex catalysts. Control of solid structure and π-conjugation length. *Macromol. Chem. Phys.* **1999**, *200*, 265−282.

(53) Uemura, T.; Kitaura, R.; Ohta, Y.; Nagaoka, M.; Kitagawa, S. Nanochannel-promoted polymerization of substituted acetylene in porous coordination polymers. *Angew. Chem., Int. Ed.* **2006**, *45*, 4112−4116.

(54) Uemura, T.; Horike, S.; Kitagawa, S. Polymerization in coordination nanospaces. *Chem. - Asian J.* **2006**, *1*, 36−44.

(55) Kageyama, K.; Tamazawa, J.-I.; Aida, T. Extrusion polymerization: catalyzed synthesis of crystalline linear polyethylene nanofibers within a mesoporeous silica. *Science* **1999**, *285*, 2113−2115.

(56) Ke, Z.; Abe, S.; Ueno, T.; Morokuma, K. Rh-catalyzed polymerization of phenylacetylene: theoretical studies of the reaction mechanism, regioselectivity, and stereoregularity. *J. Am. Chem. Soc.* **2011**, *133*, 7926−7941.

(57) Liu, J. Z.; Lam, J. W. Y.; Tang, B. Z. Acetylenic polymers: syntheses, structures, and functions. *Chem. Rev.* **2009**, *109*, 5799−5867.

(58) Castanon, J. R.; Sano, N.; Shiotsuki, M.; Sanda, F. Synthesis of poly(1-chloro-2-arylacetylene)s with high cis-content and examination of their absorption/emission properties. *J. Polym. Sci., Part A: Polym. Chem.* **2017**, *55*, 382−388.

(59) Cobos, K.; Rodríguez, R.; Domarco, D.; Fernández, B.; Quinoá, E.; Riguera, R.; Freire, F. Polymeric helical structures à la carte by rational design of monomers. *Macromolecules* **2020**, *53*, 3182−3193.

(60) Prieto, G.; Tüysüz, H.; Duyckaerts, N.; Knossalla, J.; Wang, G.-H.; Schüth, F. Hollow Nano- and Microstructures as Catalysts. *Chem. Rev.* **2016**, *116*, 14056−14119.